Observational Study

Microstructural Abnormalities in Gray Matter of Patients with Postherpetic Neuralgia: A Diffusional Kurtosis Imaging Study

Yi Zhang, MD, Tian Yu, MD, Bangyong Qin, MD, Ying Li, MD, Ganjun Song, BSMT, and Buwei Yu, MD

From: Ruijin Hospital, Shanghai Jiaotong University School of Medicine, Shanghai, China

Address Correspondence:
Buwei Yu, MD
Department of Anesthesiology
Rui Jin Hospital
No.197,Rui Jin Er Roa
Shanghai 200025 China
E-mail: pact12345@163.com

Disclaimer: There was no external funding in the preparation of this manuscript. Conflict of interest: Each author certifies that he or she, or a member of his or her immediate family, has no commercial association (i.e., consultancies, stock ownership, equity interest, patent/licensing arrangements, etc.) that might pose a conflict of interest in connection with the submitted manuscript.

Manuscript received: 08-21-2015
Revised manuscript received: 10-06-2015 and 11-07-2015
Accepted for publication: 11-20-2015

Free full manuscript:
www.painphysicianjournal.com

Background: Changes in functional activity and connectivity have been shown in patients experiencing postherpetic neuralgia (PHN) pain. However, PHN-induced structural changes, particularly in the gray matter of which volume and density was widely reported to be altered by other chronic pain, have not been well characterized.

Objective: In this study, we aimed to detect the difference in the microstructure of gray matter of PHN patients as compared to the healthy controls, and to analyze the correlation between microstructural alterations and clinical features of PHN patients.

Study Design: Observational study.

Setting: University hospital.

Methods: Diffusional kurtosis imaging (DKI) was performed in 19 patients with PHN and in 19 age- and gender-matched healthy controls. Maps of axial kurtosis (K//), mean kurtosis (MK), radial kurtosis (K⊥) in gray matter were calculated and compared between the 2 groups. Correlations between kurtosis metrics in the regions where between-group difference was detected and pain intensity as well as lesion duration were tested by Pearson's correlation.

Results: Compared with healthy controls, PHN patients exhibited significantly decreased DKI parameters in the bilateral insula and superior temporal gyrus, left middle frontal gyrus and occipital lobe, right cerebellum anterior lobe, right thalamus, caudate and parahippocampal gyrus. K// in the bilateral insula and MK in the right insula were negatively correlated with visual analogue scale (VAS) scores of PHN patients, whereas no correlation was found between DKI parameters and lesion duration of PHN pain.

Limitation: Relatively small sample size. We still cannot determine the causal and effect relationship between the microstructural abnormalities in the gray matter and PHN.

Conclusions: DKI can specifically reflect pathophysiological microstructural alterations in the cerebral gray matters of PHN patients. This feature enables magnetic resonance imaging (MRI) to be a potentially valuable technique for objectively estimating the severity of PHN pain, which would provide an opportunity for elucidating the central mechanisms underlying PHN as well.

Key words: Postherpetic neuralgia, diffusional kurtosis imaging, insula cortex, gray matter, voxel-based analysis

Pain Physician 2016; 19:E601-E611

Postherpetic neuralgia (PHN) is the most common complication of herpes zoster (HZ). In PHN patients, pain persists in the infected regions for months or even years after the HZ rash heals, which affects the life quality of patients and elicits anxiety and depression, particularly in the elderly (1,2). As a typical chronic neuropathic pain, PHN produces various neuropathic signs in both the peripheral and

central nervous system (3). Yet few studies have focused on the effects of PHN on brain functional activity using functional magnetic resonance imaging (fMRI) (4,5). These results indicated that brain regions in association with sense, hedonics, reward, and punishment were activated by spontaneous PHN. In addition, increased cerebral blood flow (CBF) was found in the striatum, thalamus, primary somatosensory cortex, insula, amygdala, and inferior parietal lobule, and decreased CBF was found in the frontal cortex (6). However, comparing with the progress made in functional imaging studies, the changes of the cerebral structure in patients with PHN are still poorly understood.

It has been suggested that chronic pain other than PHN may affect brain structures, especially in the gray matter (GM) (7). Using voxel-based morphometry (VBM), changes in the global and regional GM volume and density were observed in patients with chronic back pain (8), burning mouth syndrome (9), migraine (10), fibromyalgia (11), and trigeminal neuralgia (12), etc. However, whether PHN will also induce microstructural changes in the GM of patients is still not well known (13).

Diffusion-based MRI has long been used to assess the tissue microstructure in the brain non-invasively. Conventional MRI techniques, such as diffusion tensor imaging (DTI), are based on the assumption that the diffusion of water molecules is Gaussian (14). However, factually a variety of tissue structures in the brain restrict free water diffusion, which results in the deviation of diffusion from the Gaussian behavior (15). As an extension of conventional DTI, diffusional kurtosis imaging (DKI) is a novel diffusion imaging technique that has been developed to characterize the non-Gaussianity of water diffusion (16), and thus offers more comprehensive and sensitive information of tissue microstructural changes in the brain (17,18). Compared with DTI that are appropriate for cerebral white matter (WM) studies, DKI could more effectively quantify the microstructural abnormalities in GM, due to the isotropic water diffusion in GM (19). This sensitivity to GM is important in the studies on the microstructural alterations induced by chronic pain conditions, in consideration of the widely reported alteration in GM.

In the present study, we hypothesize that PHN induces microstructural abnormalities in the cerebral GM of patients. To test this hypothesis, we employed DKI to detect the difference in the GM microstructure of PHN patients as compared to healthy controls, and then to assess the relationship between microstructural alterations in the corresponding regions and clinical features of PHN patients.

Methods

Participants

The current study was approved by the Ethics Committee of our local hospital, and written informed consent was obtained from all participants. Right-handed PHN patients admitted to the pain clinic of our local hospital were recruited in our study. The diagnosis of PHN was based on the International Association for the Study of Pain (IASP) criteria for postherpetic neuralgia (20). The intensity levels of spontaneous pain was assessed using a visual analog scale (VAS), with a range from 0 (no pain) to 10 (most intense pain imaginable). All PHN patients in our study reported persistent pain for more than 2 months (2 – 24 months) after their HZ rash healed, with a pain intensity of at least 5/10 on VAS. No participant had a history of psychiatric or neurological disorder. The MRI scanning was implemented on the day of hospital admission and before the systematic treatment in the hospital. A standard anatomical brain scan was performed first. Patients with visible neurological abnormalities were not enrolled in our study. Finally data from 19 PHN patients were analyzed: 9 men and 10 women, 13 patients with left-sided lesions and 6 patients with right-sided lesions, ranging in age from 46 to 72 (mean 62.5 years). Nineteen age-, gender-matched right-handed healthy volunteers (8 men and 11 women, ranging in age from 46 to 68) were recruited as the control group. All volunteers in the control group were free of pain conditions, brain structural abnormalities, and neuropsychiatric disorders.

Image Acquisition

All MRI experiments were implemented on a GE Signa HDxT 3.0 T MRI scanner (General Electric Medical System, USA) with a standard 8-channel head coil. MRI scans and preliminary evaluation of images were performed by an experienced neuroradiologist. For each patient, earplugs were used to reduce the scanner noise. Three b-values (0, 1000, and 2000 s/mm2) and diffusion encoding vectors along 25 nonparallel directions for each nonzero b-value were applied in the current study. DKI images were acquired by a spin-echo single-shot echo planar imaging (EPI) sequence with parameters as follow: repetition time (TR)/echo time (TE) = 10000/99.3 ms, slice thickness = 4 mm, gap = 0, flip angle = 15°, slice thickness = 4 mm, field of view (FOV)

= 240 mm × 240 mm, matrix = 128 × 128 and scan time = 530 s. In addition, T1 weighted images (3-dimensional brain volume imaging, 3D-BRAVO) were obtained with the following parameters: TR/TE = 7.8/3, inversion time (TI) = 450 ms, FOV = 256 mm × 256 mm, matrix = 256 ×256, slice = 1 mm, slice gap = 0 mm, number of signal averages (NEX) = 1, flip angle = 15°, bandwidth = 31.25 Hz, scan time = 208s.

Image Processing

Image processing and analysis were implemented by another experienced neuroradiologist. All DICOM files were first converted to NIFTI format. Eddy-current distortion and head motion were corrected using FSL (FMRIB Software Library, Oxford, UK) (21). The toolkit DKE (22) based on MATLAB R2012a (Math Works Inc., Sherborn, MA, USA) was applied to estimate the DKI parametric maps, including the mean, axial, and radial kurtosis (MK, K//, K⊥).

For voxel-based analysis (VBA), all the parametric images were processed by the following steps: First, b0 images of all patients were normalized to the standard EPI template in SPM8 with a reslicing resolution of 3 mm × 3 mm × 3 mm. The normalized b0 images were averaged and smoothed with an 8 mm full-width-at-half-maximum (FWHM) Gaussian kernel to generate the b0 template. Subsequently, all parametric maps including K//, K⊥, MK, and each original b0 image were normalized to the b0 template with a reslicing resolution of 3mm × 3mm × 3mm. The normalized images were smoothed with an 8 mm FWHM Gaussian kernel as well. To generate a GM mask, a T1 weighted image of each patient was segmented into GM, WM, and cerebrospinal fluid (CBF) in its original resolution using SPM8. The acquired GM images were then normalized to the standard Montreal Neurological Institute (MNI) space with a reslicing resolution of 3 mm × 3 mm × 3 mm. The normalized GM images of each patient were averaged and smoothed with an 8 mm FWHM Gaussian kernel, and then converted into binary masks that overlaid on the DKI parametric maps for further GM analysis.

Statistical Analysis

Demographic and clinical data were analyzed using SPSS software (v.19.0.1, IBM, USA). Two-sample t-tests were used for detecting the differences in the age, VAS scores and pain duration between PHN patients and health controls. $\chi 2$ test was applied for comparison of gender. The criteria for all statistical significance was $P < 0.05$.

VBA was performed for only GM on normalized and smoothed K//, K⊥, and MK maps using Statistical Parametric Mapping (SPM8, Wellcome Department of Imaging Neuroscience, London, UK) based on MATLAB. A two-sample t-test was applied to determine the difference between groups. Combination of voxel with $P < 0.001$ and cluster size > 13 voxel produced a corrected threshold of $P < 0.05$, which was determined by AlphaSim software (http://afni.nih.gov/afni/docpdf/AlphaSim.pdf).

Brain regions showing significant differences ($P < 0.05$, corrected) in the values of DKI parameters between the 2 groups were extracted as the regions of interest (ROI) masks. Thereafter these ROI masks were projected onto the normalized and smoothed images of each PHN patient, and the values of DKI parameters in the ROIs were estimated and extracted. The correlation between regional DKI parameters and VAS score, and between parameters and pain duration were determined using Pearson's correlation, with $P < 0.05$ (two-tailed) considered as statistically significant.

Results

Demographic and Clinical Features

Clinical characteristics of PHN patients are shown in Table 1. There were no remarkable differences in age (62.53 ± 7.62 vs 59 ± 7.67, $P = 0.164$) and gender (F/M = 9/10 vs 8/11, $P = 0.744$) between PHN patients and healthy controls.

Comparison of DKI Parameters between Two Groups

As shown in Table 2 and Fig. 1, patients with PHN showed significantly decreased K// mainly in the bilateral insula and superior temporal gyrus, left middle frontal gyrus and occipital lobe, right cerebellum anterior lobe, right thalamus, caudate, and parahippocampal gyrus. Lower MK was observed in the bilateral insula, right superior temporal gyrus, thalamus, caudate, and parahippocampal gyrus (Table 3 and Fig. 2). Regions with decreased K⊥ included the left insula, right caudate, thalamus, and right parahippocampal gyrus (Table 4 and Fig. 3). No regions with higher K//, K⊥, and MK were detected.

Correlation between DKI Parameters and Clinical Variables

The above regions with decreased K//, K⊥, and MK were respectively extracted as ROI for correlation

Table 1. *Clinical characteristics of PHN patients.*

NUM	Age(y)	Gender	Location of lesion	Pain duration (month)	VAS score
1	61	F	Left T10-12	3	6
2	71	F	Left T1-4	2	5
3	53	M	Right V1-2	3	6
4	70	M	Left T1-2	24	5
5	64	F	Left T5-7	18	6
6	67	F	Right T12-L1	5	7
7	68	M	Right C8-T2	3	7
8	61	M	Left T1-3	5	7
9	57	F	Right T1-5	5	7
10	67	M	Left C2-4	3	7
11	59	M	Left L2-3	6	5
12	72	F	Left T2-4	3	5
13	46	F	Left V1-2	3	8
14	61	M	Left L2-3	2	5
15	48	F	Right V1	5	5
16	70	M	Left C1-4	3	7
17	69	M	Left S3-4	3	7
18	66	F	Left C2-4	2	8
19	58	F	Right V2	2	5

M = male; F = female; T = level of thoracic vertebrae; L: level of lumbar vertebrae;
S: level of sacral vertebrae; V1, V2: ophthalmic and maxillary branches of the trigeminal nerve

Table 2. *Clusters of significant difference in axial kurtosis (K//).*

NO.	Anatomical location	MNI coordinate			Cluster size	Peak t value
		x	y	z		
1	Superior Temporal Gyrus_L	-53	5	-3	198	-4.23
2	Superior Temporal Gyrus_R	57	-9	0	77	-3.4
3	Insula_L	-42	-12	6	155	-5.86
4	Insula_R	42	-6	-6	85	-4.94
5	Cerebellum Anterior Lobe_R	9	-50	-4	137	-4.51
6	Thalamus_R	5	-9	15	85	-4.28
7	Caudate_R	6	16	3	58	-4.8
8	Parahippocampal Gyrus_R	21	6	21	54	-4.84
9	Occipital Lobe_L	-5	-64	1	65	-4.52
10	Middle Frontal Gyrus_L	-33	51	-6	131	-4.57

L: left, R: right, MNI: Montreal Neurological Institute

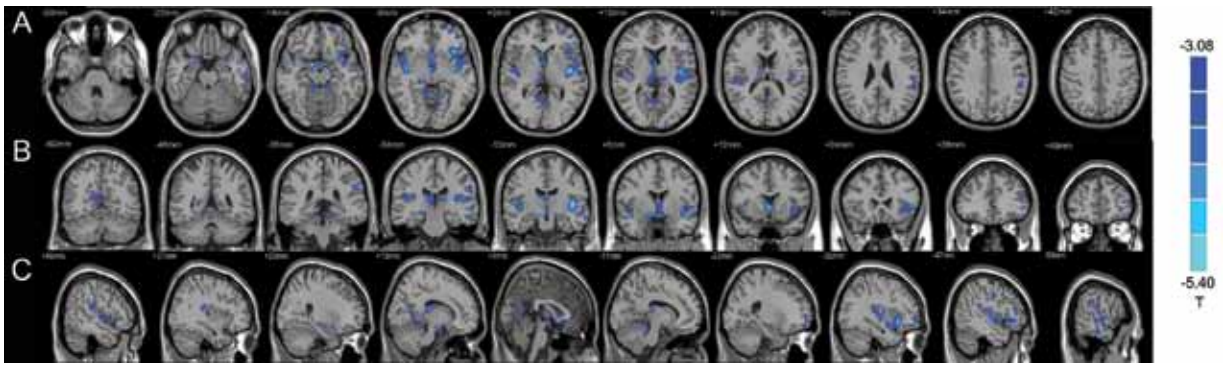

Fig. 1. *Significant differences in K// between PHN patients and healthy controls in axial (A), coronal (B), and sagittal (C) slices. Statistical differences are shown superimposed in color on a standard Montreal Neurological Institute (MNI) template. The blue regions indicate significantly lower K// in PHN patients than healthy controls (P < 0.05, corrected). The MNI coordinates are used for location in all directions. T-values are color-coded on the right. Left in the figure represents the right side of patients.*

Table 3. *Clusters of significant difference in mean kurtosis (MK).*

NO.	Anatomical location	MNI coordinate			Cluster size	Peak t value
		x	y	z		
1	Thalamus_R	12	-27	12	64	-3.89
2	Parahippocampal Gyrus_R	18	2	-25	56	-5.11
3	Insula_L	-41	-13	3	127	-4.97
4	Superior Temporal Gyrus_R	54	5	-9	58	-3.19
5	Insula_R	45	6	-9	51	-4.17
6	Caudate_R	6	16	2	64	-4.76

L: left, R: right, MNI: Montreal Neurological Institute

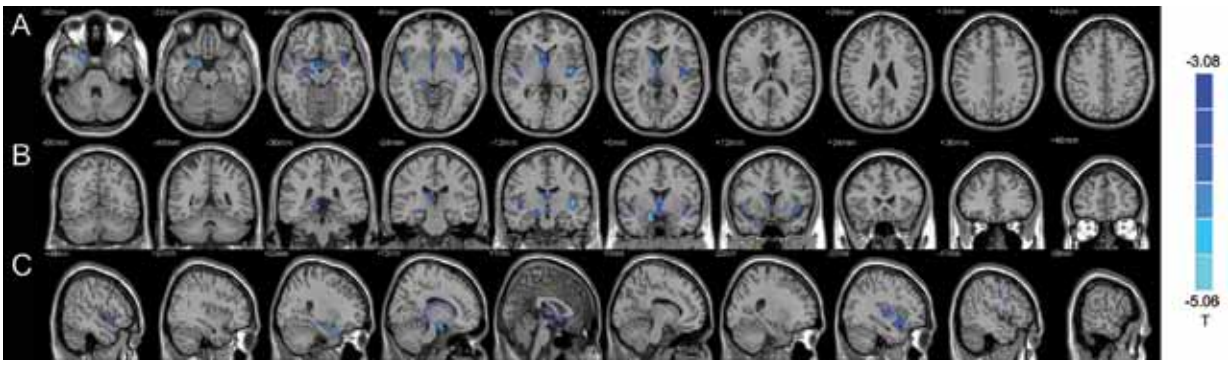

Fig. 2. *Significant differences in MK between PHN patients and healthy controls in axial (A), coronal (B), and sagittal (C) slices. Statistical differences are shown superimposed in color on a standard MNI template. The blue regions show significantly lower MK in PHN patients than healthy controls (P < 0.05, corrected). The MNI coordinates are used for location in all directions. T-values are color-coded on the right. Left in the figure represents the right side of patients.*

analysis with VAS scores and lesion duration. As shown in Fig. 4, the K// value in the bilateral insula and the MK value in the right insula were negatively correlated with VAS scores of PHN patients. However, no correlation was detected between DKI parameters in ROI and lesion duration of PHN.

Discussion

Alteration of GM volume or density in the brain has been widely reported to be tightly associated with chronic pain (9,12,23-26), although it is still debated whether structural reorganization in the brain is part of the cause or only the consequence of the pain. Rather than measuring the gross changes in GM volume/density by VBM, recently a DTI study has demonstrated the microstructural tissue abnormalities in the GM of patients with trigeminal neuralgia, and also the changes of DTI parameters in specific brain regions were found to be correlated with pain relief following treatment (27). In the present study, the microstructural changes in the relatively isotropic GM could be better characterized with the DKI method.

In the primary DKI parameters, MK reflects the complexity of tissue microstructure and degree of diffusion restriction, while K// and K⊥ provide directionally specific information on the kurtosis parallel and perpendicular to the principal diffusion tensor eigenvector, of which K// reflects axonal integrity, whereas K reflects myelin integrity (28). In the GM of PHN patients, we observed that all the 3 DKI parameters decreased in different brain regions. These regions include the bilateral insula and superior temporal gyrus, left middle frontal gyrus and occipital lobe, right cerebellum anterior lobe, right thalamus, caudate, and parahippocampal gyrus. In these regions, the thalamus, insula, and prefrontal cortex are the so-called pain matrix (13,29), which was defined as the common areas involved in pain perception regardless of the location, duration, or nature of pain. The thalamus is the area related to sensory processes. Functional activities in the thalamus can be intensively affected by spontaneous pain and tactile allodynia of PHN (5,30). Also patients with other chronic neuropathic pain have shown reduced GM volume in the bilateral thalamus (31,32). In the current study, the

Table 4. *Clusters of significant difference in radial kurtosis (K⊥).*

NO.	Anatomical location	MNI coordinate			Cluster size	Peak t value
		x	y	z		
1	Caudate_R	6	12	7	54	-4.17
2	Parahippocampal Gyrus _R	21	5	-26	53	-5.12
3	Thalamus_R	4	-21	6	51	-3.8
4	Insula_L	-40	-12	4	76	-4.69

L: left, R: right, MNI: Montreal Neurological Institute

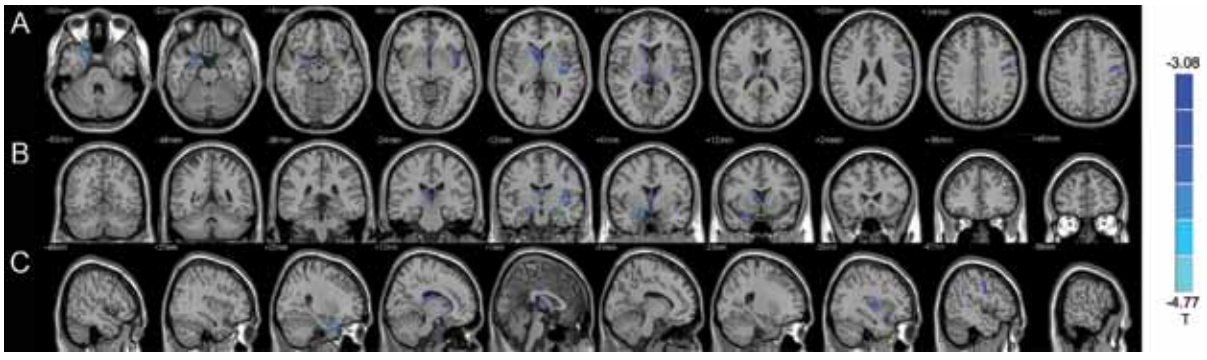

Fig. 3. *Significant differences in K⊥ between PHN patients and healthy controls in axial (A), coronal (B), and sagittal (C) slices. Statistical differences are shown superimposed in color on a standard MNI template. The blue regions show significantly lower K⊥ in PHN patients than healthy controls (P < 0.05, corrected). The MNI coordinates are used for location in all directions. T-values are color-coded on the right. Left in the figure represents the right side of patients.*

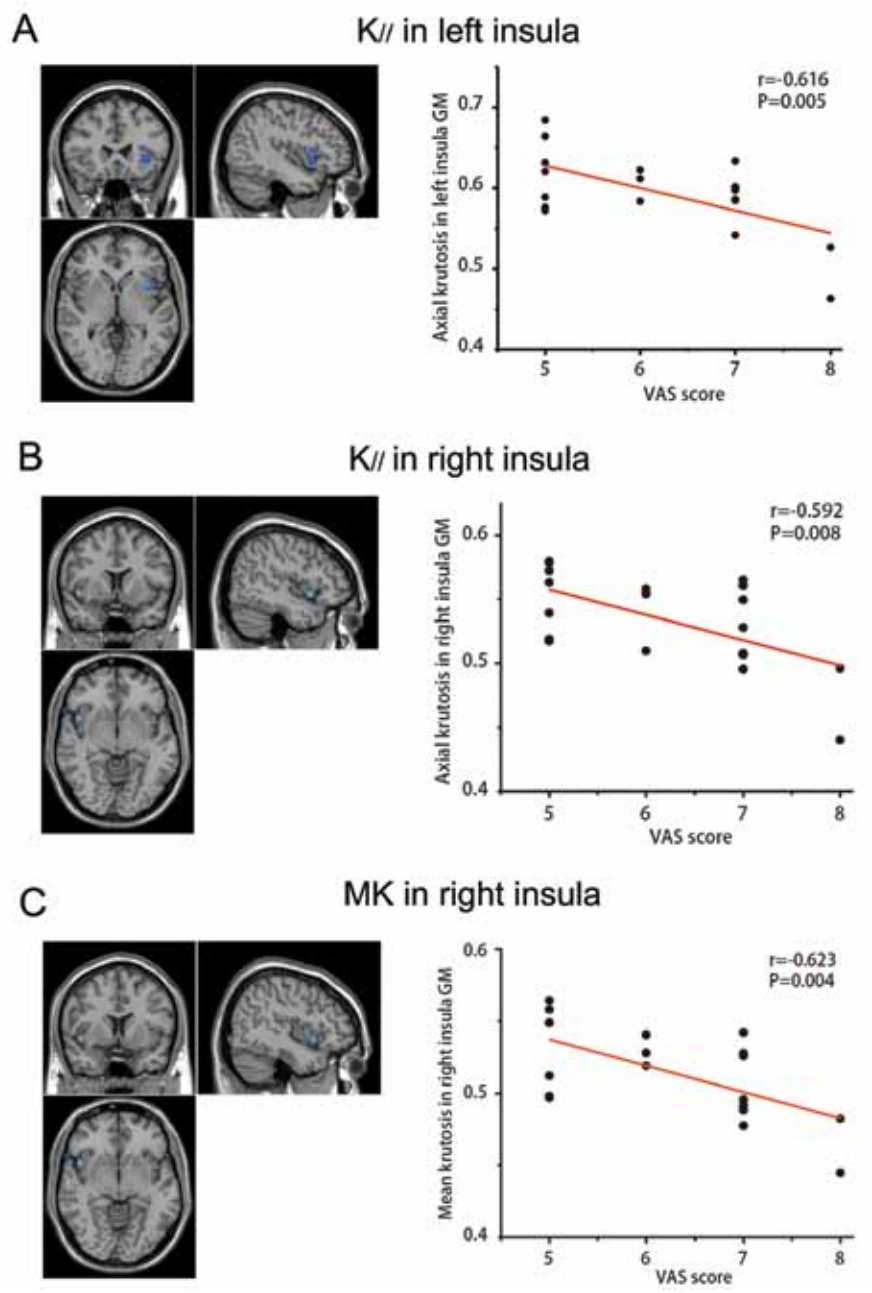

Fig. 4. *Correlation analysis between DKI parameters and VAS scores. Panel A and B show that the K// value in the left and right insula are negatively correlated with VAS scores of PHN patients. C: the MK value in the right insula is negatively correlated with VAS scores as well.*

3 primary DKI parameters all decreased in the right thalamus, exhibiting strongly the involvement of thalamic microstructural abnormalities in PHN pain. The middle frontal gyrus is implicated in emotion modulation and executive function (33). Decreased low-frequency fluctuation (ALFF) and GM volume/density

in the middle frontal gyrus were reported in patients with irritable bowel syndrome (24,34). Consistent with these reports, our data demonstrate the notably abnormal tissue microstructure in the middle frontal gyrus, which is presumably implicated in the emotional aspect of PHN pain. The insula cortex plays an important role in integrating sensory information and generating subjective emotional experience (35). Patients with chronic somatic and visceral pain showed remarkable reduced GM volume in the insula cortex (36,37). Equally, our data indicate significantly decreased DKI parameters in the insula. More specially, correlation analysis in our study indicated that the values of K// and MK in the insula were negatively correlated with pain intensity of PHN. This result emphasized the vulnerability and sensitivity of microstructure abnormalities of the insula in PHN pain, which is supported by the previous functional (38,39) and structural (23,40) studies.

The caudate, one part of the striatum, is involved in the hedonics, emotion, and rewards, while the parahippocampal gyrus links tightly to memory/affective process. K//, K⊥, and MK in our study all showed a significant decrease in both the caudate and parahippocampal gyrus, suggesting strongly that the 2 regions are severely affected by PHN pain. This result is consistent with the previous findings of PHN observed using fMRI (4,6). In addition, reduced GM volume in the parahippocampal gyrus found in patients with other chronic pain supports our results as well (41,42). Therefore, it is conceivable that microstructural abnormalities in the caudate and parahippocampal gyrus might account for the corresponding behavioral consequence in the emotion and memory aspect of PHN pain. Other regions where notable decreased DKI parameters were detected include the temporal gyrus and occipital lobe, along with the cerebellum. Consistent with our observation, patients experiencing other chronic pain such as cluster headache, chronic low back pain, and migraine also show gray matter loss in these regions in the previous VBM studies (43-45).

In GM, kurtosis can be influenced by alteration in tissue water content and cell packing density, changes in cytoarchitecture, as well as addition of basal dendrites (46-48). In our study, K//, MK, and K⊥ were lower in PHN patients to a varying extent. More regions with decreased K// were probed rather than MK and K⊥ (Table 2 and Fig. 1), and the decrease of K// in the insula was highly correlated with VAS score (Fig. 4 A and B). These results suggested that the microstructural complexity was remarkably reduced in all the diffusion directions, of which K// is more sensitive to detect the microstructural abnormalities induced by PHN.

Generally, the pathological mechanisms underlying decreased MK may be associated with the myelin deficiency, neuronal edema, and increased permeability in the neuron membranes in local brain regions (49,50). Lower K// is associated with a decrease in packing density of fiber bundles and axons, changes in neurofibrils or decreased extracellular complexity along the axial direction, while decreased K⊥ is mainly ascribed to demyelination or axonal loss that bring about less restriction in the radial direction (51). Together, combined with the shrunken GM volume reported in the previous literature, our results implied that the lesions in the GM of PHN patients may be primarily characterized by architectural alteration in basal dendritic spines and reduced packing density of nerve fibers along the axial direction.

Long-term pain widely affects brain anatomy primarily via the cerebral adaptation mechanism to frequent nociceptive inputs with regard to neural plasticity (52). Moreover, altered regional CBF by PHN pain may account for the structural abnormalities as well. It has been suggested that frontal cerebral perfusion is associated with GM volume in heroin addiction (53). Similarly, in line with the results from CBF alterations of PHN patients utilizing arterial spin labeling (ASL) techniques (6), altered microstructures were also detected in the insula, thalamus, and frontal cortex in our study. In these regions, long-term changes in perfusion induced by chronic pain may underlie the reorganization of neural tissue, such as neuronal degeneration and proliferation of astrocytes and microglia (54). In turn, the microstructural abnormalities examined in the present study probably contribute to the developmental process and the consequent clinical manifestations of PHN. For instance, changes of tissue structures in the somatosensory and insula cortex affect processing and modulation of sensory information, and thus presumably result in the sensory deficits (55). Additionally, abnormalities in the thalamus may be the structural basis exacerbating the disinhibition of nociceptive inputs, which will induce allodynia (56,57). Chronic pain-induced subtle alterations in the prefrontal cortex lead to changes in an individual's personality (58). Therefore, these microstructural abnormalities revealed in our study may be implicated in the central mechanism of PHN pain, and account for the long-term persistence of pain states (43,59).

In the current study, there is no significant correlation between lesion duration of PHN patients and DKI

parameter. However, it has been reported that neural plasticity in GM following chronic pain is time-dependent in the previous VBM studies. For instance, reduced GM volume and density was positively correlated with the lesion time of chronic pain (60,61). We speculate this inconsistency may be due to the maldistribution of lesion duration. Most of PHN patients in our study had lesion duration of less than 6 months. The reason is that the incidence of visible neurological abnormalities such as demyelination in standard anatomical brain MRI scans was much higher in PHN patients with pain duration of more than 6 months. Thus, most of the patients with long pain duration more than 6 months were excluded as the current study only focuses on the microstructural changes that cannot be detected in the anatomical scanning.

There are some limitations in the present study. Firstly, although DKI can detect the microstructural abnormalities non-invasively and more specifically, to date the unique method to clarify the pathological alterations underlying the decrease of DKI parameters is still histopathological analysis. Secondly, it still cannot be determined whether the microstructural abnormalities in GM are the result or cause of PHN, and whether these changes can be reversed after PHN pain relief. Further longitudinal studies are required to address the corresponding causal and effect relationship. Finally, both HZ and PHN are sharp pain, and thus all the patients in our study had taken one or more irregular medications for treating HZ and reliving the intense pain of PHN before hospital admission. However, the current sample size is not enough to classify and analyze the complicated situation of their medications. Future studies might be need to estimate the efficacy of different therapies or medications using the DKI method.

Conclusions

Using the DKI method, we found that PHN patients displayed subtle GM abnormalities in the brain regions related to sensory, emotional, and affective processes, in particular along the axonal direction. A significant negative correlation between DKI parameters in the insula and PHN pain intensity was found as well. These results may help to improve the assessment and treatment of patients with PHN. On the other hand, DKI can provide specific characterization of microstructural alterations in neural tissue, and thus has potentially great value in objectively estimating the severity of PHN pain, which also would provide an in-depth insight into the central mechanisms underlying PHN.

References

1. Cadogan MP. Herpes zoster in older adults. *Journal of Gerontological Nursing* 2010; 36:10-14.
2. Pickering G, Leplege A. Herpes zoster pain, postherpetic neuralgia, and quality of life in the elderly. *Pain Practice* 2011; 11:397-402.
3. Oaklander AL. The density of remaining nerve endings in human skin with and without postherpetic neuralgia after shingles. *Pain* 2001; 92:139-145.
4. Zhang Y, Liu J, Li L, Du M, Fang W, Wang D, Jiang X, Hu X, Zhang J, Wang X, Fang J. A study on small-world brain functional networks altered by postherpetic neuralgia. *Magnetic Resonance Imaging* 2014; 32:359-365.
5. Geha PY, Baliki MN, Chialvo DR, Harden RN, Paice JA, Apkarian AV. Brain activity for spontaneous pain of postherpetic neuralgia and its modulation by lidocaine patch therapy. *Pain* 2007; 128:88-100.
6. Liu J, Hao Y, Du M, Wang X, Zhang J, Manor B, Jiang X, Fang W, Wang D. Quantitative cerebral blood flow mapping and functional connectivity of postherpetic neuralgia pain: A perfusion fMRI study. *Pain* 2013; 154:110-118.
7. Borsook D, Erpelding N, Becerra L. Losses and gains: Chronic pain and altered brain morphology. *Expert Review of Neurotherapeutics* 2013; 13:1221-1234.
8. Ivo R, Nicklas A, Dargel J, Sobottke R, Delank KS, Eysel P, Weber B. Brain structural and psychometric alterations in chronic low back pain. *European Spine Journal* 2013; 22:1958-1964.
9. Khan SA, Keaser ML, Meiller TF, Seminowicz DA. Altered structure and function in the hippocampus and medial prefrontal cortex in patients with burning mouth syndrome. *Pain* 2014; 155:1472-1480.
10. Kim JH, Suh SI, Seol HY, Oh K, Seo WK, Yu SW, Park KW, Koh SB. Regional grey matter changes in patients with migraine: A voxel-based morphometry study. *Cephalalgia* 2008; 28:598-604.
11. Burgmer M, Gaubitz M, Konrad C, Wrenger M, Hilgart S, Heuft G, Pfleiderer B. Decreased gray matter volumes in the cingulo-frontal cortex and the amygdala in patients with fibromyalgia. *Psychosomatic Medicine* 2009; 71:566-573.
12. Obermann M, Rodriguez-Raecke R, Naegel S, Holle D, Mueller D, Yoon MS, Theysohn N, Blex S, Diener HC, Katsarava Z. Gray matter volume reduction reflects chronic pain in trigeminal neuralgia. *NeuroImage* 2013; 74:352-358.
13. May A. Chronic pain may change the structure of the brain. *Pain* 2008; 137:7-15.
14. Basser PJ, Pierpaoli C. Microstructural and physiological features of tissues elucidated by quantitative-diffusion-tensor MRI. *Journal of Magnetic Resonance* 1996; 111:209-219.
15. Lu H, Jensen JH, Ramani A, Helpern JA. Three-dimensional characterization of non-gaussian water diffusion in humans using diffusion kurtosis imaging.

NMR in Biomedicine 2006; 19:236-247.

16. Jensen JH, Helpern JA, Ramani A, Lu H, Kaczynski K. Diffusional kurtosis imaging: The quantification of non-gaussian water diffusion by means of magnetic resonance imaging. *Magnetic Resonance in Medicine* 2005; 53:1432-1440.
17. Cheung MM, Hui ES, Chan KC, Helpern JA, Qi L, Wu EX. Does diffusion kurtosis imaging lead to better neural tissue characterization? A rodent brain maturation study. *NeuroImage* 2009; 45:386-392.
18. Jensen JH, Helpern JA, Tabesh A. Leading non-Gaussian corrections for diffusion orientation distribution function. *NMR in Biomedicine* 2014; 27:202-211.
19. Hori M, Tsutsumi S, Yasumoto Y, Ito M, Suzuki M, Tanaka FS, Kyogoku S, Nakamura M, Tabuchi T, Fukunaga I, Suzuki Y, Kamagata K, Masutani Y, Aoki S. Cervical spondylosis: Evaluation of microstructural changes in spinal cord white matter and gray matter by diffusional kurtosis imaging. *Magnetic Resonance Imaging* 2014; 32:428-432.
20. Merskey H, Bogduk N. *Classification of Chronic Pain: Descriptions of Chronic Pain Syndromes and Definitions of Pain Terms.* Ed 2. International Association for the Study of Pain, Seattle, 1994.
21. Smith SM, Jenkinson M, Woolrich MW, Beckmann CF, Behrens TE, Johansen-Berg H, Bannister PR, De Luca M, Drobnjak I, Flitney DE, Niazy RK, Saunders J, Vickers J, Zhang Y, De Stefano N, Brady JM, Matthews PM. Advances in functional and structural MR image analysis and implementation as FSL. *NeuroImage* 2004; 23:S208-S219.
22. Tabesh A, Jensen JH, Ardekani BA, Helpern JA. Estimation of tensors and tensor-derived measures in diffusional kurtosis imaging. *Magnetic Resonance in Medicine* 2011; 65:823-836.
23. Lutz J, Jager L, de Quervain D, Krauseneck T, Padberg F, Wichnalek M, Beyer A, Stahl R, Zirngibl B, Morhard D, Reiser M, Schelling G. White and gray matter abnormalities in the brain of patients with fibromyalgia: A diffusion-tensor and volumetric imaging study. *Arthritis and Rheumatism* 2008; 58:3960-3969.
24. Labus JS, Dinov ID, Jiang Z, Ashe-McNalley C, Zamanyan A, Shi Y, Hong JY, Gupta A, Tillisch K, Ebrat B, Hobel S, Gutman BA, Joshi S, Thompson PM, Toga AW, Mayer EA. Irritable bowel syndrome in female patients is associated with alterations in structural brain networks. *Pain* 2014; 155:137-149.
25. Buckalew N, Haut MW, Morrow L, Weiner D. Chronic pain is associated with brain volume loss in older adults: Preliminary evidence. *Pain Medicine* 2008; 9:240-248.
26. Desouza DD, Moayedi M, Chen DQ, Davis KD, Hodaie M. Sensorimotor and pain modulation brain abnormalities in trigeminal neuralgia: A paroxysmal, sensory-triggered neuropathic pain. *PLoS One* 2013; 8:e66340.
27. DeSouza DD, Davis KD, Hodaie M. Reversal of insular and microstructural nerve abnormalities following effective surgical treatment for trigeminal neuralgia. *Pain* 2015; 156:1112-1123.
28. Hui ES, Cheung MM, Qi L, Wu EX. Towards better MR characterization of neural tissues using directional diffusion kurtosis analysis. *NeuroImage* 2008; 42:122-134.
29. Moisset X, Bouhassira D. Brain imaging of neuropathic pain. *NeuroImage* 2007; 37:S80-S88.
30. Geha PY, Baliki MN, Wang X, Harden RN, Paice JA, Apkarian AV. Brain dynamics for perception of tactile allodynia (touch-induced pain) in postherpetic neuralgia. *Pain* 2008; 138:641-656.
31. Barad MJ, Ueno T, Younger J, Chatterjee N, Mackey S. Complex regional pain syndrome is associated with structural abnormalities in pain-related regions of the human brain. *The Journal of Pain* 2014; 15:197-203.
32. Maeda Y, Kettner N, Sheehan J, Kim J, Cina S, Malatesta C, Gerber J, McManus C, Mezzacappa P, Morse LR, Audette J, Napadow V. Altered brain morphometry in carpal tunnel syndrome is associated with median nerve pathology. *NeuroImage* 2013; 2:313-319.
33. Schoenbaum G, Roesch M. Orbitofrontal cortex, associative learning, and expectancies. *Neuron* 2005; 47:633-636.
34. Ma X, Li S, Tian J, Jiang G, Wen H, Wang T, Fang J, Zhan W, Xu Y. Altered brain spontaneous activity and connectivity network in irritable bowel syndrome patients: A resting-state fMRI study. *Clinical Neurophysiology* 2015; 126:1190-1197.
35. Cauda F, D'Agata F, Sacco K, Duca S, Geminiani G, Vercelli A. Functional connectivity of the insula in the resting brain. *NeuroImage* 2011; 55:8-23.
36. Seminowicz DA, Labus JS, Bueller JA, Tillisch K, Naliboff BD, Bushnell MC, Mayer EA. Regional gray matter density changes in brains of patients with irritable bowel syndrome. *Gastroenterology* 2010; 139:48-57; e42.
37. Pan PL, Zhong JG, Shang HF, Zhu YL, Xiao PR, Dai ZY, Shi HC. Quantitative meta-analysis of grey matter anomalies in neuropathic pain. *European Journal of Pain* 2015; 19:1224-1231.
38. Ichesco E, Schmidt-Wilcke T, Bhavsar R, Clauw DJ, Peltier SJ, Kim J, Napadow V, Hampson JP, Kairys AE, Williams DA, Harris RE. Altered resting state connectivity of the insular cortex in individuals with fibromyalgia. *The Journal of Pain* 2014; 15:815-826; e811.
39. Baliki MN, Mansour AR, Baria AT, Apkarian AV. Functional reorganization of the default mode network across chronic pain conditions. *PLoS One* 2014; 9:e106133.
40. Farmer MA, Chanda ML, Parks EL, Baliki MN, Apkarian AV, Schaeffer AJ. Brain functional and anatomical changes in chronic prostatitis/chronic pelvic pain syndrome. *The Journal of Urology* 2011; 186:117-124.
41. Schmidt-Wilcke T, Leinisch E, Straube A, Kampfe N, Draganski B, Diener HC, Bogdahn U, May A. Gray matter decrease in patients with chronic tension type headache. *Neurology* 2005; 65:1483-1486.
42. Kuchinad A, Schweinhardt P, Seminowicz DA, Wood PB, Chizh BA, Bushnell MC. Accelerated brain gray matter loss in fibromyalgia patients: Premature aging of the brain? *The Journal of Neuroscience* 2007; 27:4004-4007.
43. Obermann M, Wurthmann S, Steinberg BS, Theysohn N, Diener HC, Naegel S. Central vestibular system modulation in vestibular migraine. *Cephalalgia* 2014; 34:1053-1061.
44. Ung H, Brown JE, Johnson KA, Younger J, Hush J, Mackey S. Multivariate classification of structural MRI data detects chronic low back pain. *Cerebral Cortex* 2014; 24:1037-1044.
45. Naegel S, Holle D, Desmarattes N, Theysohn N, Diener HC, Katsarava Z, Obermann M. Cortical plasticity in episodic and chronic cluster headache. *NeuroImage* 2014; 6:415-423.
46. Bockhorst KH, Narayana PA, Liu R, Ahobila-Vijjula P, Ramu J, Kamel M, Wosik J, Bockhorst T, Hahn K, Hasan KM, Perez-Polo JR. Early postnatal development of rat brain: In vivo diffusion tensor imaging. *Journal of Neuroscience Research* 2008; 86:1520-1528.
47. Huppi PS, Dubois J. Diffusion tensor imaging of brain development. *Semi-*

nars in Fetal & Neonatal Medicine 2006; 11:489-497.

48. Mukherjee P, Miller JH, Shimony JS, Philip JV, Nehra D, Snyder AZ, Conturo TE, Neil JJ, McKinstry RC. Diffusion-tensor MR imaging of gray and white matter development during normal human brain maturation. *AJNR* 2002; 23:1445-1456.
49. Zhang Y, Yan X, Gao Y, Xu D, Wu J, Li Y. A preliminary study of epilepsy in children using diffusional kurtosis imaging. *Clinical Neuroradiology* 2013; 23:293-300.
50. Gong NJ, Wong CS, Chan CC, Leung LM, Chu YC. Correlations between microstructural alterations and severity of cognitive deficiency in Alzheimer's disease and mild cognitive impairment: A diffusional kurtosis imaging study. *Magnetic Resonance Imaging* 2013; 31:688-694.
51. Wu EX, Cheung MM. MR diffusion kurtosis imaging for neural tissue characterization. *NMR in Biomedicine* 2010; 23:836-848.
52. Woolf CJ, Salter MW. Neuronal plasticity: Increasing the gain in pain. *Science* 2000; 288:1765-1769.
53. Denier N, Schmidt A, Gerber H, Schmid O, Riecher-Rossler A, Wiesbeck GA, Huber CG, Lang UE, Radue EW, Walter M, Borgwardt S. Association of frontal gray matter volume and cerebral perfusion in heroin addiction: A multimodal neuroimaging study. *Frontiers in Psychiatry* 2013; 4:135.
54. Shibata M, Ohtani R, Ihara M, Tomimoto H. White matter lesions and glial activation in a novel mouse model of chronic cerebral hypoperfusion. *Stroke* 2004; 35:2598-2603.
55. Davis KD, Taylor KS, Anastakis DJ. Nerve injury triggers changes in the brain. *The Neuroscientist* 2011; 17:407-422.
56. Cesaro P, Mann MW, Moretti JL, Defer G, Roualdes B, Nguyen JP, Degos JD. Central pain and thalamic hyperactivity: A single photon emission computerized tomographic study. *Pain* 1991; 47:329-336.
57. Cecchi GA, Huang L, Hashmi JA, Baliki M, Centeno MV, Rish I, Apkarian AV. Predictive dynamics of human pain perception. *PLoS Computational Biology* 2012; 8:e1002719.
58. Gustin SM, McKay JG, Petersen ET, Peck CC, Murray GM, Henderson LA. Subtle alterations in brain anatomy may change an individual's personality in chronic pain. *PLoS One* 2014; 9:e109664.
59. Kuner R. Central mechanisms of pathological pain. *Nature Medicine* 2010; 16:1258-1266.
60. Draganski B, Moser T, Lummel N, Ganssbauer S, Bogdahn U, Haas F, May A. Decrease of thalamic gray matter following limb amputation. *NeuroImage* 2006; 31:951-957.
61. Absinta M, Rocca MA, Colombo B, Falini A, Comi G, Filippi M. Selective decreased grey matter volume of the pain-matrix network in cluster headache. *Cephalalgia* 2012; 32:109-115.